ANALYSIS ON SHIELDING PERFORMANCE OF METALLIC RECTANGULAR CASCADED ENCLOSURE WITH APERTURES

G. Wu, X.-G. Zhang, Z.-Q. Song, and B. Liu

China Academy of Space Technology
Xi'an 710100, Shaanxi, China

Abstract—A full-wave approach is proposed to evaluate the shielding performance of metallic rectangular double-stage cascaded enclosures with apertures. The analysis has been carried out by means of the mode-matching technique and the mixed potential integral equation solved with the Method of Moments. The effects of the dimension of enclosures, the orientation of apertures, the polarization direction of the incident wave, the aperture thickness and the high-order modes propagating in enclosures are taken into account. The accuracy of the proposed approach is validated by comparing with other methods and numerical simulation results can derive some conclusions: the shielding performance of cascaded enclosures is better than that of single-stage enclosures, the shielding effectiveness can be improved with increasing the distance between stages in the range, and the shielding performance of the double-stage enclosure with parallel-pattern apertures in horizontal polarization case is better than that in vertical polarization case.

1. INTRODUCTION

In order to protect an electronic system from the interferences of external electromagnetic waves, metallic enclosures have been often employed to suppress its directive radiation effects. Unfortunately, some apertures have to be opened on its wall for signal connecting, power supply, and heat dispersion in practical applications. What is more, these apertures create coupling paths that allow the outside electromagnetic energy to penetrate into the enclosure and then cause the inner field resonance and the shielding performance being degraded.

Generally, the shielding performance of a metallic enclosure can be described by its shielding effectiveness (SE) which is defined as the ratio of the electromagnetic field without the present of the enclosure to the field with the present of the enclosure at the same observation point [1]. Many theoretical and experimental researches have been carried out to analyze the shielding performance of metallic single-stage enclosures with apertures irradiated by the external electromagnetic waves [2–5]. However, it should be mentioned that, due to complicated inner resonances of the structure, it is very difficult to achieve high shielding performance for a metallic single-stage enclosure. Therefore, metallic multistage cascaded enclosures could provide a better solution for the target of achieving the high shielding performance, which is our motivation behind this academic paper.

The shielding effectiveness of metallic rectangular cascaded enclosure with apertures can be analyzed using the numerical or the analytical methods. Numerical methods, such as the Method of Moments (MoM) [6], can model enclosures with sufficient detail but often requires large computing time and memory. In addition, the analytical approaches based on various simplifying assumptions [7] are also subject to many severe limitations even though providing a much faster means.

This paper proposes a rigorous full-wave solution which combines the mode-matching technique and the mixed potential integral equation based on the Method of Moments to analyze the shielding effectiveness of the metallic rectangular cascaded enclosure with apertures. Some influence factors, such as the dimension of enclosures, the orientation of apertures, the polarization direction of the incident wave, the aperture thickness and the high-order modes propagating in enclosures, are considered.
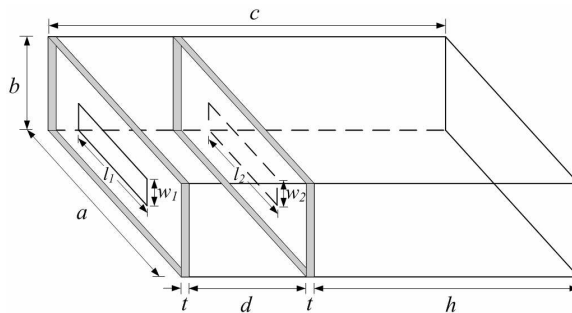

Figure 1. Geometry of rectangular double-stage cascaded enclosure with apertures.

2. THEORETICAL MODEL

The attention is focused on a metallic rectangular double-stage cascaded enclosure with two rectangular apertures illuminated by the electromagnetic wave, and its 3-D geometry is shown in Figure 1. The metallic enclosure of dimensions $a \times b \times c$ has two front walls which are assumed perfectly conducting planes with thickness t. The outer aperture $w_1 \times l_1$ is on the first wall and the inner aperture $w_2 \times l_2$ is on the second wall. The distance between the front walls is d and the length of the inner enclosure is h.

The problem can be separated into two problems by employing Schelkunoff's field equivalent principle: the interior and the exterior problems illustrated in Figure 2. The interior problem is composed of I, II, III and IV regions which can be regarded as some rectangular waveguides, while the exterior problem is considered as a half free space (V region) with an equivalent magnetic current and an incident electromagnetic wave.

3. MATHEMATICAL FORMULATION

As shown in Figure 2, the rectangular waveguides in the interior problem can be modeled using mode-matching technique, while the magnetic field in the exterior problem can be expressed by a mixed potential integral equation which is solved by the Method of Moments.
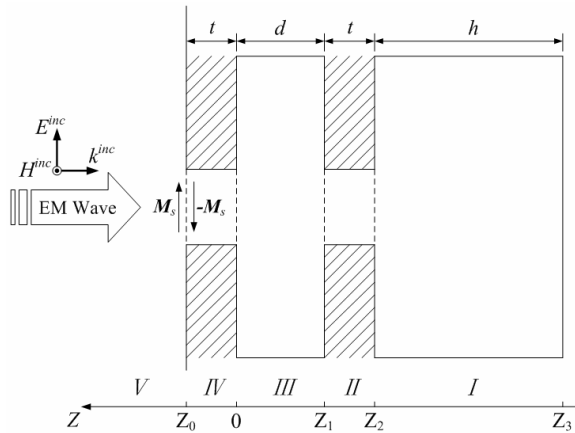

Figure 2. Equivalent model for aperture replaced by magnetic current.

3.1. Interior Problem

In order to solve the Maxwell's equations conveniently, the electric and the magnetic vector potentials are introduced whose the z-direction component is A_{ez} and A_{hz} respectively. Then the tangential electromagnetic fields in the region i $(i = I, II, III, IV)$ can be expressed as [8]:

$$\mathbf{E}_t^i = -\nabla_t A_{hz}^i \times z + \frac{1}{j\omega\varepsilon}\nabla_t \frac{\partial A_{ez}^i}{\partial z} \tag{1}$$

$$\mathbf{H}_t^i = \nabla_t A_{ez}^i \times z + \frac{1}{j\omega\mu}\nabla_t \frac{\partial A_{hz}^i}{\partial z} \tag{2}$$

$$A_{hz}^i(x, y, z) = \sum_{q=1}^{N} Q_{hq}^i T_{hq}^i \left[A_{hq}^{i+} e^{-\Gamma_{hq}^i z} + A_{hq}^{i-} e^{\Gamma_{hq}^i z} \right] \tag{3}$$

$$A_{ez}^i(x, y, z) = \sum_{q=1}^{N} Q_{eq}^i T_{eq}^i \left[A_{eq}^{i+} e^{-\Gamma_{eq}^i z} - A_{eq}^{i-} e^{\Gamma_{eq}^i z} \right] \tag{4}$$

where ε is permittivity of free space and μ is magnetic permeability of free space, T_e and T_h are the eigenfunctions of the TM (e) and TE (h) modes, respectively. In the same way, A_e and A_h are the modal amplitude coefficients, Γ_e and Γ_h are the propagation constants, Q_e and Q_h are the normalized factors such that the power carried by each mode is 1 Watt. q is the mode index.

On the assumption that there are N TM modes and N TE modes propagating in the waveguides, the $2N \times 1$ modal amplitude coefficients matrices of the positive and the negative z-direction modes in the waveguide i — A^{i+} and A^{i-} can be described as:

$$A^{i+} = \left[\begin{array}{c} A_e^{i+} \\ A_h^{i+} \end{array} \right] \quad A^{i-} = \left[\begin{array}{c} A_e^{i-} \\ A_h^{i-} \end{array} \right] \tag{5}$$

In terms of the tangential electric field and the tangential magnetic field components matching at the boundary between region I and region II respectively, the coupling matrices M whose size is $2N \times 2N$ is obtained in [9]. Then the S parameter matrix is derived as:

$$S|_{Z=0} = \left[\begin{array}{cc} -M & U \\ U & M^T \end{array} \right]^{-1} \left[\begin{array}{cc} M & -U \\ U & M^T \end{array} \right] \tag{6}$$

U is the $2N \times 2N$ unit matrix; M^T is the transpose of M. Similarly, the S parameter matrix of the waveguides junction $Z = Z_2$ is denoted by:

$$S|_{Z=Z_2} = \left[\begin{array}{cc} S_{11} & S_{12} \\ S_{21} & S_{22} \end{array} \right] \tag{7}$$

The generalized scattering matrix is independent of the coordinates, therefore we can obtain:

$$S|_{Z=Z_1} = \begin{bmatrix} S_{22} & S_{21} \\ S_{12} & S_{11} \end{bmatrix} \tag{8}$$

On account of the waveguides i is equivalent to the finite transmission lines, the S parameter matrix of the waveguide i is educed:

$$S|_{i\,region} = \begin{bmatrix} 0 & D \\ D & 0 \end{bmatrix} \tag{9}$$

where $D|_{i\,region} = \mathrm{diag}\{\exp(-\Gamma_q^i d^i)\}$, d^i is the length of the waveguide i, $i = II, III$.

The total S parameter matrix S_{tot} of the complicated structure between the region I and region IV can be analyzed by cascading the aforementioned S parameter matrices. And then from the Equation (10) the total coupling matrix M_{tot} is obtained.

$$M_{tot}^T = S_{tot21}(U - S_{tot11})^{-1} \tag{10}$$

Therefore, the relationship of the modal amplitude coefficients in the region I and the region IV can be shown:

$$A^{I+} + A^{I-} = M_{tot}(A^{IV+} + A^{IV-}) \tag{11}$$

$$M_{tot}^T(A^{I+} - A^{I-}) = A^{IV+} - A^{IV-} \tag{12}$$

On account of the end of the waveguide I is considered as a short circuit, the propagating waves along $-z$ direction can be reflected completely, then the relationship of the modal amplitude coefficients in region I is described as:

$$A^{I+} = -L^I A^{I-} \tag{13}$$

where $L^I = \mathrm{diag}\{e^{-2\Gamma_j^I h}\}$, $j = e, h$. Substituting (13) into (11) and (12) gives a matrix equation describing the relationship of the modal amplitude coefficients in region IV:

$$A^{IV+} = \rho A^{IV-} \tag{14}$$

where

$$\rho = (U + P)^{-1}(U - P)$$
$$P = M_{tot}^T(L^I + U)(U - L^I)^{-1}M_{tot}^T$$

Substituting (13) and (14) into (11) and (12) gives a matrix equation:

$$A^{I-} = (U - L^I)^{-1}M_{tot}^T(\rho + U)A^{IV-} \tag{15}$$

3.2. Exterior Problem

In Figure 2, the plane $Z = Z_0$ is considered as an infinite conductive plane. According to the equivalence principle, the aperture whose area is Sa on the plane $Z = Z_0$ can be replaced by the equivalent surface magnetic current $\mathbf{M}_s$, which is given by [10]:

$$\mathbf{M}_s = -\mathbf{n} \times \mathbf{E}_t^{IV}(t) \tag{16}$$

with $\mathbf{n}$ being the normal unit vector pointing outwards.

By means of image theory, the equivalent magnetic current $2\mathbf{M}_s$ substitutes as the equivalent source for the half-space. Mathematically, the magnetic field $\mathbf{H}^{Ms}$ due to $2\mathbf{M}_s$ in the Region V can be written as follows:

$$\mathbf{H}^{M_S} = -j\omega \mathbf{F}(\mathbf{r}) - \nabla\phi_m(\mathbf{r}) \tag{17}$$

The inner product is defined by:

$$\langle A, B \rangle = \iint_{sa} A \cdot B dS \tag{18}$$

where the integration extends over the aperture on the plane $z = t$ for the 2D case. Then the electric vector potential $\mathbf{F}$ and the magnetic scalar potential ϕ_m at a field point $\mathbf{r}$ are given by:

$$\mathbf{F}(\mathbf{r}) = 2\varepsilon \left\langle \mathbf{M}_s(\mathbf{r}'), \overset{\rightarrow F}{\overset{\rightarrow}{\mathbf{G}}}_{free}(\mathbf{r}|\mathbf{r}') \right\rangle \tag{19}$$

$$\phi_m(\mathbf{r}) = \frac{2j}{\omega\mu} \left\langle \nabla'_t \cdot \mathbf{M}_s(\mathbf{r}'), G_{free}^{\phi_m}(\mathbf{r}|\mathbf{r}') \right\rangle \tag{20}$$

$\overset{\rightarrow F}{\overset{\rightarrow}{\mathbf{G}}}_{free}$ and $G_{free}^{\phi_m}$ are the dyadic and the scalar Green's function for the free space respectively.

3.3. Operation of Matrix Equations

According to the continuity of the tangential magnetic field through the aperture on the plane $z = t$, the magnetic formulation can be accomplished by enforcing:

$$\mathbf{H}_t^{M_S} + 2\mathbf{H}_t^{inc} = \mathbf{H}_t^{II}(t) \tag{21}$$

The Equation (21) can be solved by MoM, and then the equivalent magnetic current $\mathbf{M}_s$ is expanded by a set of the vectorial basis functions $\mathbf{W}_n$ with unknown coefficients K_n as:

$$\mathbf{M}_s = \sum_{n=1}^{2N} K_n \cdot \mathbf{W}_n \tag{22}$$

Moreover, the Galerkin procedure is applied. Setting the weighting function $\mathbf{W}$ $(2N \times 1)$ equal to the basis function as:

$$\mathbf{W} = \left[\begin{array}{c} \mathbf{W}_e \\ \mathbf{W}_h \end{array} \right] = \left[\begin{array}{c} \frac{\Gamma_e^{IV}}{j\omega\varepsilon} Q_e^{IV} (\nabla_t T_e^{IV}) \times z \\ -Q_h^{IV} (\nabla_t T_h^{IV}) \end{array} \right] \tag{23}$$

In terms of the orthogonality of expansion functions, the mixed potential integral Equation (21) can be transformed into the following matrix equation:

$$TK + I^{inc} = Z \tag{24}$$

where

$$TK = -j\omega\langle \mathbf{W}, \mathbf{F} \rangle - \langle \mathbf{W}, \nabla\phi_m \rangle = -j\omega\langle \mathbf{W}, \mathbf{F} \rangle + \langle \nabla_t \mathbf{W}, \phi_m \rangle$$
$$K = L^{IV} A^{IV+} + (L^{IV})^{-1} A^{IV-}$$
$$I^{inc} = \langle \mathbf{W}, 2\mathbf{H}_t^{inc} \rangle$$
$$Z = \langle \mathbf{W}, \mathbf{H}_t^{IV} \rangle = L^{IV} A^{IV+} - (L^{IV})^{-1} A^{IV-}$$
$$L^{IV} = \mathrm{diag}\left\{ e^{-\Gamma_j^{IV} t} \right\} \quad j = e, h$$

And then from (14) together with (24), the unknown modal coefficients A^{IV-} is readily obtained if the incident plane wave has been given:

$$A^{IV-} = \left[\left(L^{IV}\rho - (L^{IV})^{-1} \right) - T \left(L^{IV}\rho + (L^{IV})^{-1} \right) \right]^{-1} I^{inc} \tag{25}$$

Finally, Substituting (25) into the matrix Equations (15) and (13), all the modes propagating in the region I can be calculated. The field strength at any point in the metallic rectangular double-stage cascaded enclosure with apertures can be evaluated consequently.

4. NUMERICAL RESULTS

For the validation of the present technique, we consider a typical rectangular enclosure with dimensions $(30\,\mathrm{cm} \times 12\,\mathrm{cm} \times 35.3\,\mathrm{cm})$ and two parallel rectangular apertures of size $(10\,\mathrm{cm} \times 0.5\,\mathrm{cm})$ with thickness $t = 1.5\,\mathrm{mm}$ located at the center of the front walls with distance $d = 5\,\mathrm{cm}$ as shown in Figure 1. The incident plane wave is propagating along negative z-direction and its polarization is vertical polarization (the direction of the electric field is parallel to the short edge of the apertures). The observation point is located at the center of the inner enclosure whose length is $30\,\mathrm{cm}$.

The shielding effectiveness of the double-stage enclosure obtained using the present method is compared with those from FDTD method [6], and the agreement between them is observed from the Figure 3. It should be mentioned that 62 TM modes and 62 TE modes
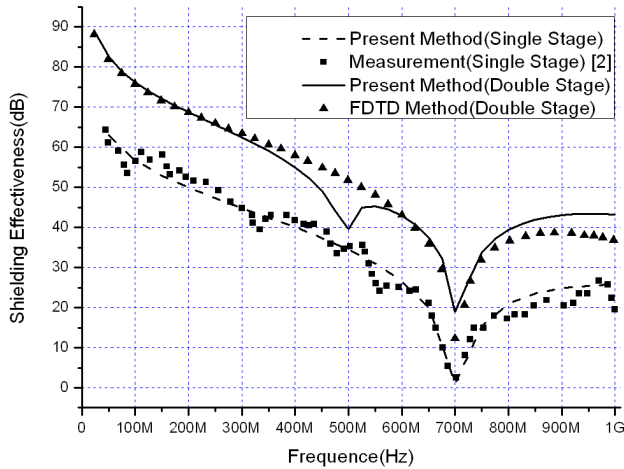
Figure 3. SE of single and double stage enclosure with $10 \times 0.5\,\text{cm}^2$ apertures.

are employed in this model. Furthermore, the shielding effectiveness of the single stage enclosure of dimensions $30\,\text{cm} \times 12\,\text{cm} \times 30\,\text{cm}$ (inner face) with the same rectangular aperture located at the center of the front wall [9] is introduced in the Figure 3. It can be seen that the dips in the shielding effectiveness are corresponding to the first resonant frequency (near $700\,\text{MHz}$) predicted at which TE_{101} mode is excited in the inner shielding enclosures, and the shielding performance of the double-stage enclosure is better than that of the single-stage enclosure.

In order to analyze the effect of varying the distance between the front walls on the shielding performance of metallic rectangular double-stage cascaded enclosure with apertures, different values of the distance d are considered, while the other parameters of this model are not changed. The results obtained for various distances are shown in Figure 4. It is found that with increasing the distance d of front walls in the range, the shielding effectiveness can be improved, mainly contributed by the attenuation of the high order modes propagating in the model.

From Figure 5, it should be pointed out that in the case of the normal incidence wave with the vertical polarization, the shielding performance of the double stage enclosure depends on the orientation of apertures on the front walls. Except for parallel-pattern apertures, two apertures could be arranged in a cross-pattern, namely the $10\,\text{cm} \times 0.5\,\text{cm}$ aperture on the first wall and the $0.5\,\text{cm} \times 10\,\text{cm}$ aperture on the second wall, and the distance of the front walls is kept as $5\,\text{cm}$. It is obvious that the value of SE for the cross-pattern aperture case

is larger than that for the parallel-pattern aperture case.

The investigation is also extended to the effect of the different polarization directions of the incident wave on the shielding performance of the metallic rectangular cascaded enclosure with apertures. The incident plane wave with the horizontal polarization (the direction of the electric field is parallel to the long edge of the outer aperture) is introduced, while the other parameters of this model are hold. It is observed that the value of SE for the cross-pattern aperture case is smaller than that of the parallel-pattern aperture case in Figure 6. In addition, it should be noted that
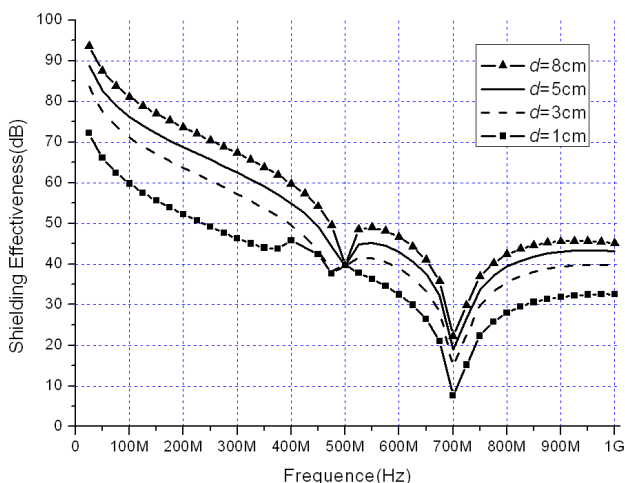

Figure 4. SE of double stage enclosure with various distances between front walls
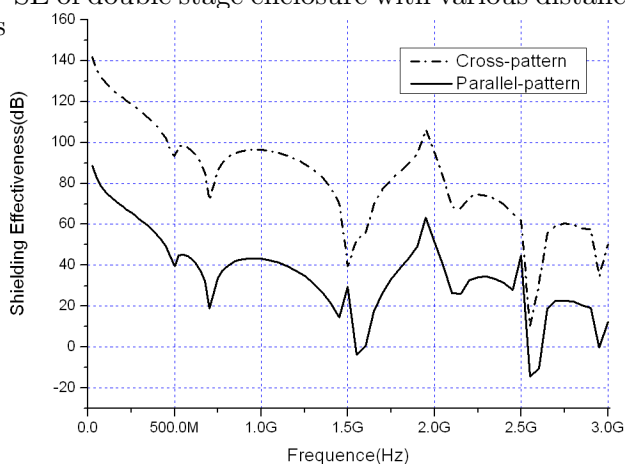

Figure 5. SE of double stage enclosure with different aperture arrangement in vertical polarization case.
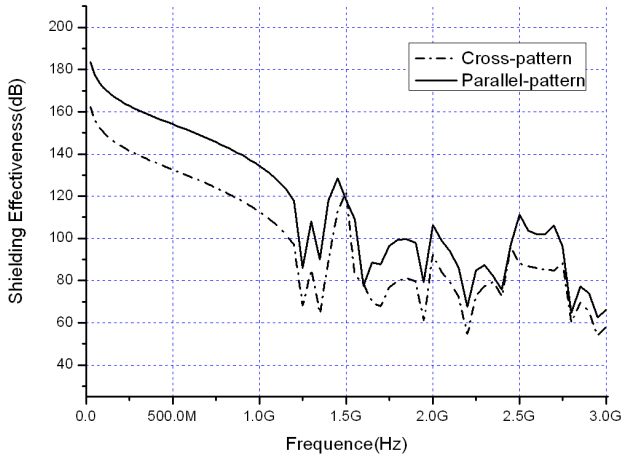
Figure 6. SE of double stage enclosure with different aperture arrangement in horizontal polarization case.

the shielding performance of the double-stage enclosure with parallel-pattern apertures in horizontal polarization case is better than that in vertical polarization case from Figures 5 and 6, but the similar conclusion of shielding performance with cross-pattern apertures is not obvious, because of the sensitivity of SE to the polarization of the incident wave.

5. CONCLUSION

In this paper, the shielding performance of metallic rectangular double-stage cascaded enclosures with apertures illuminated by external electromagnetic waves is investigated numerically. The mathematical methodology adopts the mode-matching technique and the mixed potential integral equation based on the Method of Moments, where unknown amplitude coefficients of the propagating modes in the model are solved by a set of matrix equations. This study not only gives an appropriate electromagnetic model in the development of multistage cascaded shielding structures without some uncertain approximations, but also can be further implemented in the design of electromagnetic protection for certain electronic and communication systems in the presence of high-power electromagnetic interferences.

ACKNOWLEDGMENT

REFERENCES

1. Celozzi, S., R. Araneo, and G. Lovat, *Electromagnetic Shielding*, John Wiley & Sons, Inc., New Jersey, 2008.

2. Robinson, M. P., T. M. Benson, C. Christopoulos, J. F. Dawson, M. D. Ganley, A. C. Marvin, S. J. Porter, and D. W. P. Thomas, "Analytical formulation for the shielding effectiveness of enclosures with apertures," *IEEE Trans. Electromagn. Compat.*, Vol. 40, No. 3, 240–247, 1998.

3. Lei, J.-Z., C.-H. Liang, and Y. Zhang, "Study on shielding effectiveness of metallic cavities with apertures by combining parallel FDTD method with windowing technique," *Progress In Electromagnetics Research*, Vol. 74, 85–112, 2007.

4. Araneo, R. and G. Lovat, "Fast MoM analysis of the shielding effectiveness of rectangular enclosures with apertures, metal plates, and conducting objects," *IEEE Trans. Electromagn. Compat.*, Vol. 51, No. 2, 274–283, 2009.

5. Dehkhoda, P., A. Tavakoli, and R. Moini, "Fast calculation of the shielding effectiveness for a rectangular enclosure of finite wall thickness and with numerous small apertures," *Progress In Electromagnetics Research*, Vol. 86, 341–355, 2008.

6. Xue, M. F., W. Y. Yin, Q. F. Liu, and J. F. Mao, "Wideband pulse responses of metallic rectangular multistage cascaded enclosures illuminated by an EMP," *IEEE Trans. Electromagn. Compat.*, Vol. 50, No. 4, 274–283, 2008.

7. Bahadorzadeh Ghandehari, M., M. Naser-Moghaddasi, and A. R. Attari, "Improving of shielding effectiveness of a rectangular metallic enclosure with aperture by using extra wall," *Progress In Electromagnetics Research Letters*, Vol. 1, 45–50, 2008.

8. Zhang, B. Q., "Research on mode-matching method in microwave passive component design," Ph.D. Dissertation, University of Electronic Science and Technology of China, Chengdu, 2004.

9. Wu, G., X. G. Zhang, and B. Liu, "A hybrid method for predicting the shielding effectiveness of rectangular metallic enclosures with thickness apertures," *Journal of Electromagnetic Waves and Applications*, Vol. 24, Nos. 8–9, 1157–1169, 2010.

10. Harrington, R. F., *Time-harmonic Electromagnetic Fields*, IEEE Press, New Jersey, 2001.